Raman scattering measurements of the spin ladder compound $(C_5H_{12}N)_2CuBr_4$

2005 J. Phys.: Condens. Matter 17 4237

(http://iopscience.iop.org/0953-8984/17/27/001)

INSTITUTE OF PHYSICS PUBLISHING JOURNAL OF PHYSICS: CONDENSED MATTER

J. Phys.: Condens. Matter **17** (2005) 4237–4244 doi:10.1088/0953-8984/17/27/001

Raman scattering measurements of the spin ladder compound $(C_5H_{12}N)_2CuBr_4$

K-Y Choi[1], V Gnezdilov[2], B C Watson[3], M W Meisel[3], D R Talham[4] and P Lemmens[5]

[1] Institute for Materials Research, Tohoku University, Katahira 2-1-1, Sendai 980-8577, Japan
[2] B I Verkin Institute for Low Temperature Physics NASU, 61164 Kharkov, Ukraine
[3] Department of Physics and The Center for Condensed Matter Sciences, University of Florida, PO Box 118440, Gainesville, FL 32611-8440, USA
[4] Department of Chemistry, University of Florida, PO Box 117200, Gainesville, FL 32611-7200, USA
[5] Institute for Physics of Condensed Matter, TU Braunschweig, D-38106 Braunschweig, Germany

E-mail: choi@imr.tohoku.ac.jp

Received 31 March 2005, in final form 10 June 2005
Published 24 June 2005
Online at stacks.iop.org/JPhysCM/17/4237

Abstract

We report Raman scattering measurements on the spin ladder compound $(C_5H_{12}N)_2CuBr_4$. Pronounced multiphonon scattering is observed up to eighth-order, arising from the Franck–Condon process. Furthermore, a two-magnon continuum is seen with frequencies around 18 cm^{-1} at low temperatures. Its symmetric line shape suggests a substantial hopping of triplets along the leg of the ladder. Thus, the studied system is considered to represent a two-leg ladder with coupling constants in the intermediate regime between the strong and the isotropic limit.

(Some figures in this article are in colour only in the electronic version)

1. Introduction

Recently, a considerable theoretical and experimental effort has been devoted to spin ladder systems, owing to the discovery of superconductivity in the two-leg ladder material $(La, Ca, Sr)_{14}Cu_{24}O_{41}$ [1]. In addition, spin ladder compounds exhibit exotic behaviours arising from enhanced quantum fluctuations like, for example, a ground state with a spin gap, magnetization plateaus, and quantum critical points in an external magnetic field.

Two-leg spin ladders are described by the Hamiltonian $H = J_{\parallel} \sum_{\text{leg}} S_i \cdot S_j + J_{\perp} \sum_{\text{rung}} S_i \cdot S_j$, where $J_{\parallel}$ and $J_{\perp}$ are the leg and rung couplings. The nature of the magnetic excitations depends on the ratio of the leg to the rung coupling, $J_{\parallel}/J_{\perp}$. When $J_{\perp} = 0$, two decoupled

antiferromagnetic chains are recovered where the excitations from the ground state are fractional $S = 1/2$ spinons. Upon turning on the rung coupling, a spin gap immediately opens due to a power-law decay of spin correlations [2]. This is because two fractional $S = 1/2$ spinons on each chain side are bound to an integer $S = 1$ triplet. If $J_\perp$ is dominant (the strong coupling limit), the ground state consists of spin singlets and the elementary excitations are local triplets on each rung dressed by the magnetically polarized environment [3]. In the isotropic limit, $J_\parallel/J_\perp \approx 1$, still dressed one-triplet excitations can describe the physics of the spin ladder while the spectral weight of two-triplet excitations becomes significant. A distinct feature of the excitation spectrum is the presence of a midband square-root singularity in the two-triplet continuum which is reminiscent of the upper edge of the two-spinon continuum [4]. Until now, extensive experimental studies of magnetic excitations of two-leg spin ladders have been concentrated on the isotropic limit because this doping range is realized in $Ca_{14-x}La_xCu_{24}O_{41}$ compounds [5, 6]. For a more complete understanding of the nature of magnetic excitations in spin ladders, therefore, it is necessary to study other systems with a different ratio of $J_\parallel/J_\perp$.

$(C_5H_{12}N)_2CuBr_4$ is proposed to be an example of a two-leg ladder system in the strong coupling limit with $J_\parallel = 3.8$ K and $J_\perp = 13.3$ K [7]. $(C_5H_{12}N)_2CuBr_4$ has a monoclinic crystal structure (space group $P2_1/c$), consisting of isolated $CuBr_4^{2-}$ tetrahedra cocrystallized along with the organic piperidinium cations [8]. The rung of the ladder-like structure is formed by the orbital overlap of Br ions between adjacent $CuBr_4^{2-}$ tetrahedra related by a centre of inversion along the c^* axis. The leg is mediated by weak (Br $\cdots$ Br) bonds as well as by hydrogen bonds to the organic cations along the a axis. Static susceptibility shows a broadened maximum at around 8 K and a rapid drop for temperatures below 8 K, typical for a low-dimensional spin system with a nonmagnetic ground state [7]. Magnetization measurements exhibit a universal scaling behaviour near $H_{c1} = 6.6$ T and $H_{c2} = 14.6$ T which corresponds to a transition to a gapless Luttinger liquid phase and a fully polarized state, respectively [7]. This indicates that the studied system is close to a quantum critical point. A high-frequency ESR study [9] also provides evidence for the presence of a spin singlet ground state with $\Delta_{spin} = 14$ K, which is larger than $\Delta_{spin} = 9.5$ K obtained from the analysis of the magnetization.

Raman spectroscopy has turned out to be a valuable technique to investigate the ground state as well as magnetic excitations in low-dimensional quantum spin systems through the exchange coupling mechanism of light to spins, the same process that describes the magnetic exchange [10]. In this paper, we report on Raman scattering measurements of $(C_5H_{12}N)_2CuBr_4$. The main observation is a two-magnon continuum of a rather symmetric shape extending from 12 to 26 cm^{-1}. This enables us to determine a spin gap of $\Delta_{spin} \approx 8.6$ K. Furthermore, the symmetric spectral shape gives considerable evidence that the one-triplet kinetic energy along the leg is appreciable compared to the two-triplet attraction within the rung. Thus, the studied system is described by a two-leg ladder which lies between the isotropic and the strong coupling limit.

2. Experimental details

Single crystals of $(C_5H_{12}N)_2CuBr_4$ used in this work were grown by slow evaporation of the solvent from a methanol solution of [(pipdH)Br] and $CuBr_2$ [8]. The samples were characterized by static susceptibility, ESR, and magnetization measurements [7, 9]. The single crystals are twinned. Polarized Raman scattering measurements were carried out in a quasi-backscattering geometry with 2 mW of the excitation line $\lambda = 514.5$ nm of an Ar^+ laser. The spectra were collected by using a DILOR-XY triple spectrometer and a back-illuminated CCD (charge-coupled device) detector.

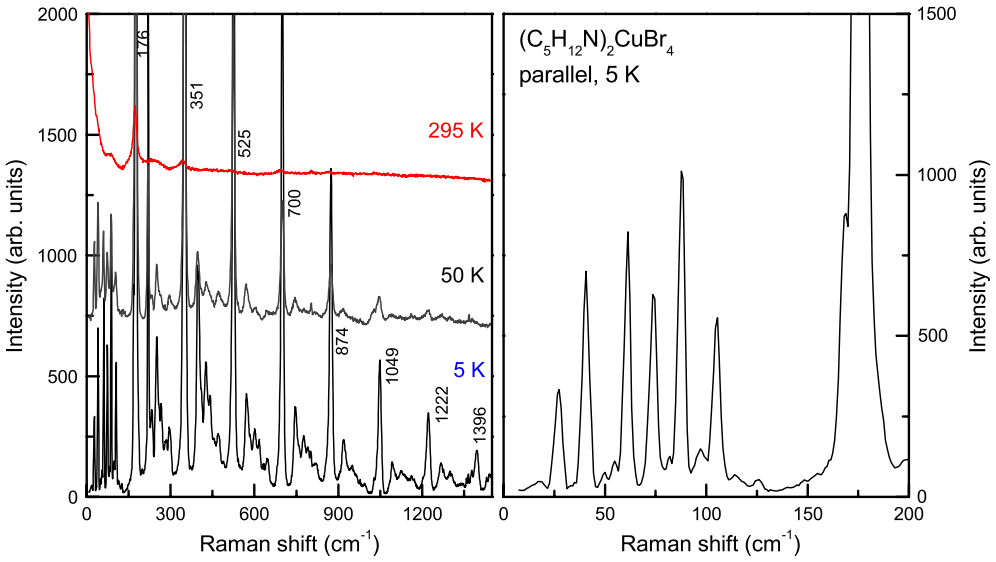

Figure 1. Left panel: polarized Raman spectra of $(Cu_5H_{12}N)_2CuBr_4$ at $T = 5, 50$, and 295 K. Multiphonon scattering is observed up to eighth order. Right panel: Magnification of one-phonon spectrum arising from the $CuBr_4^{2-}$ anions at 5 K.

3. Results and discussions

3.1. Multiphonon scattering

Shown in figure 1 are polarized Raman spectra of $(C_5H_{12}N)_2CuBr_4$ at 5, 50, and 295 K as well as a magnified spectrum of one-phonon scattering at 5 K. The title compound belongs to the space group $P2_1/c$, where all atoms have the C_1 site symmetry. For each C_1 site symmetry, we expect the following Raman- and infrared-active modes: 3 A_g(aa, bb, cc, ab) + 3 B_g(bc, ca) + 3 A_u + 3 B_u. The parentheses denote the polarization of incident and scattered light with respect to the crystallographic axis. Here we recall that the studied system consists of the $CuBr_4^{2-}$ inorganic spin ladder and the positively charged piperidinium molecules. The molecular vibrational modes of the latter are expected to show up at high frequencies of $\sim$1500 cm^{-1} while the vibrational modes of the former are given below 200–300 cm^{-1} [11].

As a result, the observed phonon scattering is exclusively governed by the $CuBr_4^{2-}$ anions. In this case, the factor group analysis of the respective anions yields $\Gamma_{Raman} =$ 15 A_g(aa, bb, cc, ab) + 15 B_g(bc, ca) Raman-active modes. For the parallel polarization of an arbitrary direction, 15 phonon modes are maximally allowed. At 5 K we observe 14 phonon modes below 176 cm^{-1}. The 176 cm^{-1} mode is assigned to the Cu–Br stretching mode (see figure 1). The remarkable thing is that phonon peaks between 176 and 299 cm^{-1} are duplicated periodically at higher frequencies. Multiphonon scattering is resolved up to eighth order. With increasing temperature the phonon modes undergo a strong damping, and their intensity decreases rapidly. Noticeably, the shift of the phonon frequencies does not exceed 2–4 cm^{-1} (not shown here). This small hardening upon cooling should be attributed to a thermal contraction arising from lattice anharmonicity. Furthermore, we find neither lattice anomalies nor evidence for structural instabilities. In this respect, our results are fully consistent with neutron diffraction and ESR studies [7, 9]. Thus, the observed strong change of the phonon

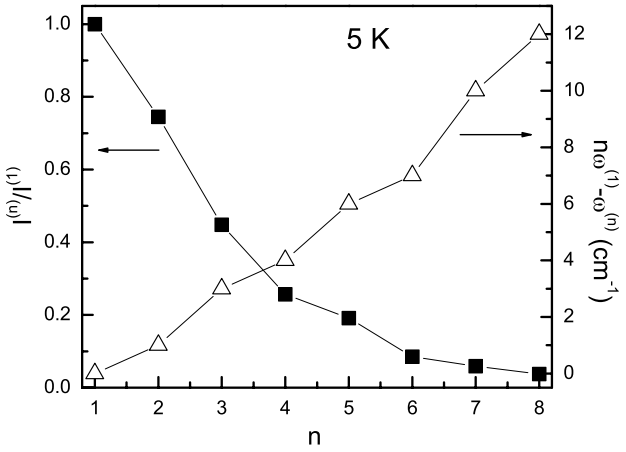

Figure 2. Normalized integrated intensity (full rectangle) and the energy difference between n-phonon scattering and integer multiples of one-phonon peak (open triangle) as a function of order n at $T = 5$ K.

intensities as a function of temperature might indicate that the Raman susceptibility tensor varies drastically with temperature due to a small modulation of the anions.

In the following, we will inspect the properties of the overtone features of the intense phonon mode at 176 cm^{-1}. Figure 2 displays the normalized intensity as a function of order (n) as well as the energy difference between n-phonon scattering and integer multiples of the one-phonon peak at 5 K. The energy difference shows a linear increase with increasing order. This means that the peak energy of n-phonon scattering systematically shifts to lower frequency upon going to higher order. This is due to a renormalization of the peak energy by phonon–phonon interactions. However, even in eighth order the energy difference of 12 cm^{-1} is small. Next, we turn to the ratio of higher- to first-order integrated phonon intensity, $I^{(n)}/I^{(1)}$, at 5 K. Noticeably, this amounts to 0.74 for $n = 2$. It falls off rapidly up to fourth order and then decreases rather slowly. At $n = 8$ it is given by 0.04. Such a large intensity of the higher-order peak is contrasted by what is expected from multiphonon scattering relying on an anharmonic electron–phonon mechanism. For such a mechanism the n-phonon scattering intensity is given by the order of 10^{-2} of the first-order one, even for $n = 2$. Furthermore, the position of the higher-order peaks deviates strongly from that of a simple integer multiple of the one-phonon peak since the whole Brillouin zone is involved in the process of higher-order phonon scattering. Thus, the origin of the pronounced multiphonon scattering in $(C_5H_{12}N)_2CuBr_4$ lies beyond lattice anharmonicity.

In molecular systems, in contrast to metal oxide systems, the electronic states of the ground and excited states can change during the Raman scattering process by virtue of phonons. In this case, the nonvanishing overlap of the vibrational wave functions between the initial and intermediate states leads to multiphonon scattering via the so-called Frank–Condon process [12]. This local mechanism based on a displacement of the intermediate state from the initial one can explain the following features: first, the higher-order peaks remain sharp and have a line width similar to the first-order peak. Second, the frequency of higher-order scattering is usually given by integer multiples of the one-phonon energy. Third, the intensity ratio, $I^{(n)}/I^{(1)}$, is of order 10^0–10^{-1} up to order $n = 5$. Therefore, we conclude that the Franck–Condon mechanism is mainly responsible for the observed multiphonon scattering.

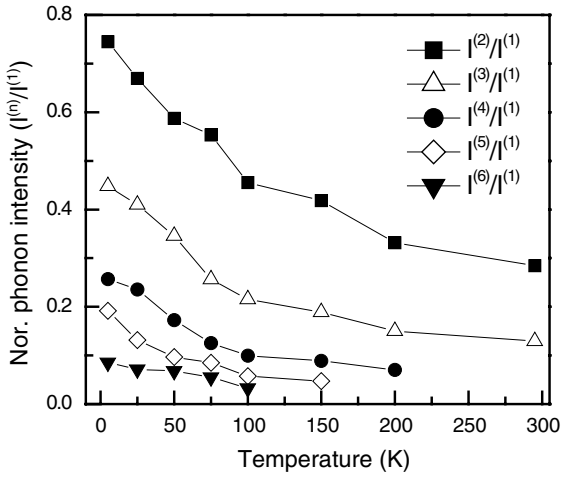

Figure 3. Temperature dependence of the normalized intensity of second-, third-, fourth-, fifth-, and sixth-order peaks.

Figure 3 shows the temperature dependence of the integrated intensity of $I^{(n)}/I^{(1)}$ ($n = 2$–6). It decreases with increasing temperature. The second-, third-, fourth-, fifth-, and sixth-order signal can be detected up to 295, 295, 200, 150, and 100 K, respectively. Here note that the temperature-dependent ratio is not consistent with the prediction of the Franck–Condon mechanism [13]. Above, we have suggested that, upon heating, the strong suppression of phonon intensities results from a substantial modulation of the optical properties by a change of the anion configuration. Actually, the $CuBr_4^{2-}$ anions are loosely coupled to each other via relatively weak Br $\cdots$ Br bonds. As a consequence, compared to the oxide system, only a small energy will be required to distort the local $CuBr_4^{2-}$ environment. This small amount of energy leads readily to the modification of the Raman tensor. In this situation, the temperature-dependent scattering intensity can be understood in terms of a variation of the overlap integral between the ground and intermediate state with temperature.

3.2. Magnetic scattering

We will now turn to the magnetic excitations observed at low temperatures and small energies compared to the phonon system. As figure 4 displays, a rather symmetric maximum centred around 18 cm^{-1} is seen at 3 K. With increasing temperature the maximum weakens in intensity while undergoing no appreciable shift of spectral weight and damping. The temperature dependence of the scattering intensity is shown in figure 5. Upon cooling down from 21 K, the intensity increases nearly linearly without saturation. This is characteristic for two-magnon scattering arising from a double spin-flip processes via the exchange mechanism within a spin-gapped system with a singlet ground state [10]. It should be noted that in classical long-range ordered systems a magnetic signal grows in intensity with a power-law behaviour and undergoes a damping and renormalization in the peak position as a function of temperature [14]. Furthermore, there is no additional signal or quasielastic scattering. This indicates that there is no substantial frustration in the exchange paths like diagonal exchange and that spin–phonon coupling is negligible.

Before proceeding further, we will consider the possible implications of twinning on the interpretation of the magnetic signals. In spin ladder systems the intensity of magnetic Raman

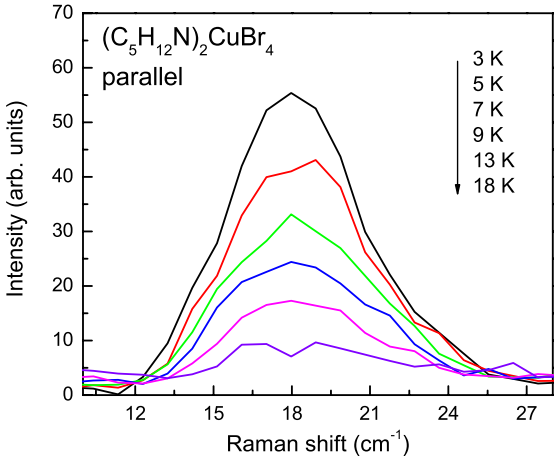

Figure 4. Temperature dependence of magnetic Raman spectra which extend from 12 to 26 cm^{-1} for low temperatures.

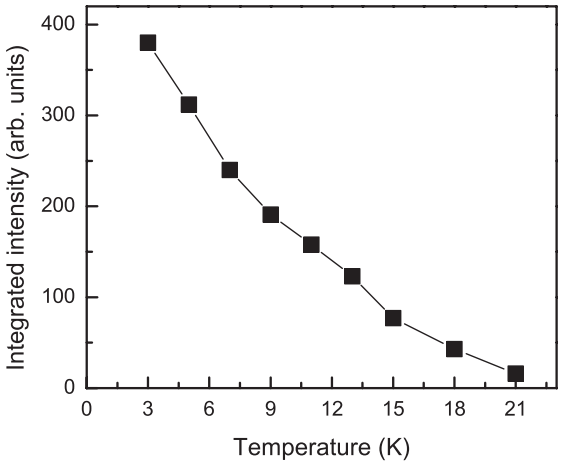

Figure 5. Temperature dependence of the integrated intensity of the magnetic continuum. With decreasing temperature the intensity increases nearly linearly without obvious saturation.

scatterings shows an angular variation depending on the respective polarization direction of incident and scattered light which are parallel to the crystallographic direction of the leg and rung of the ladder, respectively [15]. However, the scattering matrix elements do not differ from each other for both directions. This implies that the Raman line shape does not change with polarization geometry, although the scattering intensity depends on the ratio of the rung and leg exchange constants[6]. Hence, twinning does not imply an essential difficulty in extracting information from the Raman scattering signal about intrinsic magnetic properties of the system. Since our measurements are performed in a parallel configuration with respect to an arbitrary direction in the *ac* plane, the observed magnetic spectrum is an average of the signals from

[6] Strictly speaking, the Raman line shape is identical in the rung and the leg polarization only when an additional four-spin interaction is negligible and the Raman scattering is in off-resonance [16]. In contrast to the copper oxide systems, we have no evidence for the significance of a cyclic interaction in the studied system.

both the leg and rung directions. Thereby, twinning prevents the direct determination of the ratio of exchange constants. However, we can still estimate this ratio by a careful analysis of the spectral weight (described below).

First of all, we will examine the validity of a model proposed by Watson *et al* [7]. This can be easily done because in the strong coupling limit a dispersion law of local triplet excitations is given as follows [17]:

$$\omega(k) = J_\perp + J_\parallel \cos(k). \tag{1}$$

Here the spin gap is defined as the minimum excitation energy at $k = \pi$

$$\Delta_{\text{spin}} = \omega(\pi) \approx J_\perp - J_\parallel. \tag{2}$$

Since the onset of the two-magnon continuum corresponds to twice the spin gap, one can determine the spin gap of $\Delta_{\text{spin}} \approx 8.6$ K from 12 cm^{-1} (=17.2 K) (see figure 4). This value agrees well with $\Delta_{\text{spin}} \approx 9.5$ K from the analysis of the magnetization data [7] and is smaller than $\Delta_{\text{spin}} \approx 14$ K determined from ESR measurements [9]. Generally, a two-magnon continuum is given by $\omega_{2\text{mag}}(k) = \omega(k_1) + \omega(k_2)$, with $k = k_1 + k_2$. For Raman scattering this is simplified to $\omega_{2\text{mag}}(0) = 2\omega(k_1)$ since Raman spectroscopy probes total momentum-zero excitations, $k_1 \approx -k_2$. As a result, the high-energy cut-off of the two-magnon continuum corresponds to $2\omega(0) \approx 2(J_\perp + J_\parallel)$. From $2\omega(0) \approx 26$ cm^{-1}, we obtain $J_\perp = 13.7$ K and $J_\parallel = 5$ K with $J_\perp/J_\parallel = 2.74$. Our results lie in good agreement with those based on magnetization data, giving $J_\perp = 13.3$ K and $J_\parallel = 3.8$ K with $J_\perp/J_\parallel = 3.5$ [7]. This seems to confirm that the magnetic behaviour of $(C_5H_{12}N)_2CuBr_4$ is well described by a two-leg $S = 1/2$ spin ladder in the strong-coupling limit. However, this does not straightforwardly guarantee our conclusion, because in the beginning we have assumed an energy dispersion that holds only strictly in the strong coupling limit.

Thus, its relevance can be approved just after identifying that $(C_5H_{12}N)_2CuBr_4$ really represents a two-leg ladder in the strong coupling limit. We have another way to cross-check this point. For two-leg spin ladders, the line shape of Raman scattering is determined by the ratio of the exchange constants as detailed numerical calculations of Raman spectral density show [4]. In the strong coupling limit, the Raman spectrum exhibits an asymmetric line shape towards lower energy. This is due to the resonance caused by the two-triplet attraction of neighbouring triplets within the rungs. With increasing leg coupling, the kinetic energy of the relative motion of the triplets increases while the attractive interaction between triplets decreases. As a result, the Raman spectrum broadens while the resonance peak shifts to the centre of the continuum. Thus, a more symmetric line shape results. Close to the isotropic limit an additional peak appears because of an intriguing interplay between the one-triplet kinetics and the two-triplet interaction. The resulting spectrum, thus, consists of two bands.

Noticeably, the observed continuum has a rather symmetric shape in contrast to a strong asymmetric shape that is expected in the strong coupling limit (compare to figure 3 of [4]). The qualitative comparison of its spectral line shape to numerical simulations roughly yields $J_\perp/J_\parallel = 1.6$ (compare figure 4 with figure 1 of [4] and further note that the definition of the ratio, $J_\perp/J_\parallel$, is reversed in [4]). This suggests a substantial hopping of triplets along the leg. Therefore, the magnetic behaviour of the studied system lies in between the strong coupling and the isotropic limit. Experimentally, however, we cannot fix the exchange constants because an analytical expression of the energy dispersion is not known in the regime away from the strong coupling limit. One possible way is to study detwinned single crystals and then to compare the two-magnon Raman scattering intensity in the leg and the rung directions [15].

Finally, we point out that we have tried to describe the observed magnetic excitation within a simple two-leg ladder. However, the rather symmetric line shape might be ascribed to the significance of additional interactions like ring exchange interactions and interladder

interactions through hydrogen bonding of the organic cations. This remains to be pursued in future experiments.

4. Conclusions

We have presented an inelastic light scattering study on the two-leg ladder compound $(C_5H_{12}N)_2CuBr_4$. Phonon spectra are characterized by pronounced multiphonon scatterings originating from the Franck–Condon process. This is attributed to the weakly coupled anions. The magnetic excitation spectrum is typical for two-magnon scattering in a spin ladder system with a spin gap of $\Delta_{spin} = 8.6$ K. The rather symmetric spectral line shape signals the significance of the one-triplet kinetic energy along the leg.

References

[1] Dagotto E 1999 *Rep. Prog. Phys.* **62** 1525 and references therein
[2] Barnes T, Dagotto E, Riera J and Swanson E 1993 *Phys. Rev.* B **47** 3196
[3] Knetter C, Schmidt K P, Grüninger M and Uhrig G S 2001 *Phys. Rev. Lett.* **87** 167204
[4] Schmidt K P, Knetter C and Uhrig G S 2001 *Europhys. Lett.* **56** 877
[5] Windt M, Grüninger M, Nunner T, Knetter C, Schmidt K P, Uhrig G S, Kopp T, Freimuth A, Ammerahl U, Büchner B and Revcolevschi A 2001 *Phys. Rev. Lett.* **87** 127002
[6] Sugai S and Suzuki M 1999 *Phys. Status Solidi* b **215** 653
[7] Watson B C, Kotov V N, Meisel M W, Hall D W, Granroth G E, Montfrooij W T, Nagler S E, Jensen D A, Backov R, Petruska M A, Fanucci G E and Talham D R 2001 *Phys. Rev. Lett.* **86** 5168
[8] Patyal B R, Scott B L and Willett R D 1990 *Phys. Rev.* B **41** 1657
[9] Zvyagin S, Watson B C, Park J-H, Jensen D A, Angerhofer A, Brunel L C, Talham D R and Meisel M W 2002 *Preprint* cond-mat/0206001
[10] Lemmens P, Güntherodt G and Gros C 2003 *Phys. Rep.* **375** 1
[11] Nakamoto K 1997 *Infrared and Raman Spectra of Inorganic and Coordination Compounds* (New York: Wiley)
[12] Cardona M 1982 *Light Scattering in Solids II* (*Springer Topics in Applied Physics* vol 50) ed M Cardona and G Güntherodt (Berlin: Springer)
[13] Pantoja A E, Trodahl H J, Fainstein A, Pregliasco R G, Buckley R G, Balakrishnan B, Lees M R and Paul D Mck 2001 *Phys. Rev.* B **63** 132406 and references therein
[14] Cottam M G and Lockwood D J 1986 *Light Scattering in Magnetic Solids* (New York: Wiley)
[15] Freitas P J and Singh R R P 2000 *Phys. Rev.* B **62** 14113
[16] Schmidt K P, Gössling A, Kuhlmann U, Thomsen C, Löffert A, Gross C and Assmus W 2005 *Preprint* cond-mat/0503558
[17] Gopalan S, Rice T M and Sigrist M 1994 *Phys. Rev.* B **49** 8901